

Resonant tunneling in crossed electric and magnetic fields in GaAs-AlAs superlattices

W. Müller

Max-Planck-Institut für Festkörperforschung, Heisenbergstrasse 1, D-70569 Stuttgart, Germany

H. T. Grahn

Paul Drude Institut für Festkörperelektronik, Hausvogteiplatz 5-7, D-10117 Berlin, Germany

K. von Klitzing

Max-Planck-Institut für Festkörperforschung, Heisenbergstrasse 1, D-70569 Stuttgart, Germany

K. Ploog

Paul-Drude-Institut für Festkörperelektronik, Hausvogteiplatz 5-7, D-10117 Berlin, Germany

(Received 12 March 1993)

We employ time-dependent photocurrent measurements to study resonant tunneling in a magnetic field parallel to the layers in two differently coupled superlattices. The shift of the resonance between the first and the second electronic subbands is proportional to the square of the magnetic field. The shift is quantitatively in agreement with theoretical calculations, taking into account the polarization of the wave functions due to the electric field. A decrease in the tunneling times at resonance with increasing magnetic field is found in the sample with stronger coupling while the weakly coupled sample shows an increase. For the weakly coupled sample, stationary photocurrent and photoluminescence measurements are alternative but less precise methods of studying resonant tunneling in a parallel magnetic field.

I. INTRODUCTION

In the past few years there has been great interest in the effect of a magnetic field applied parallel to the tunneling barrier on the tunneling characteristics of semiconductor heterostructures. While some of the work was devoted to the study of single-barrier structures¹⁻³ most experiments were performed on double-barrier resonant tunneling structures (DBRTS).⁴⁻⁸ The transition from electric to magnetic confinement in DBRTS's with wide wells was studied in Refs. 6 and 7. In Refs. 4, 5, and 8 resonant tunneling between electronic subbands was investigated and a shift of the resonances to higher electric fields was found. However, in this case a *quantitative* agreement with theoretical calculations, if attempted,⁸ was difficult to obtain due to the complicated electric field distribution in DBRTS's. A theoretical treatment of magnetotunneling in wide-well DBRTS's was presented in Ref. 9.

In contrast to a DBRTS, where the carriers tunnel from a contact layer into a quantum well, a superlattice (SL) represents a structure where tunneling takes place between identical quantum wells. The energy levels of adjacent wells can be shifted with respect to each other by means of an external voltage applied perpendicular to the layers. In a SL embedded in *p-i-n* diode biased in the reverse direction the voltage drop is linear in space, resulting in a linear energy-voltage relationship. Therefore such a SL is an ideal structure to evaluate energy spacings and energy shifts. Furthermore, we can study the *dynamics* of the tunneling process in the SL as a function

of the applied electric field F_A by employing time-of-flight (TOF) measurements.¹⁰

In a SL without a magnetic field the tunneling probability is resonantly enhanced when subbands of adjacent wells are aligned.¹⁰⁻¹² In the presence of a parallel magnetic field ($B \perp F_A$) the resonance condition is modified. If the subband spacing is much larger than the cyclotron energy $\hbar\omega_c$ ($\omega_c = eB/m^*$) the confinement is still predominantly electric and the magnetic field mainly leads to an additional parabolic potential superimposed onto the energy levels of each quantum well. Classically this corresponds to the coupling of the transverse momentum to the motion parallel to the growth direction due to the Lorentz force. This results in a shift of the tunneling resonances to higher electric fields. Experimental results on resonant tunneling in crossed electric and magnetic fields in a GaAs-AlAs SL obtained using stationary photocurrent measurements were reported in Ref. 11.

The aim of this paper is to present a comprehensive study on resonant tunneling in crossed electric and magnetic fields in differently coupled GaAs-AlAs SL's. In our experiments we investigate two SL's with almost the same SL period. However, the barrier thickness is varied, resulting in a different coupling between adjacent wells in the two samples. The SL's are embedded in a *p-i-n* structure. We employ a TOF technique¹⁰ which allows us to study the effect of the magnetic field on the dynamics of the tunneling process. For both samples the resonance between the first and second subbands is found to shift with the square of the applied magnetic field. We compare our results with theoretical calculations taking

into account the polarization of the wave functions due to the electric field and conduction band nonparabolicities. The tunneling times at resonance are strongly modified by the magnetic field in opposite ways for different barrier thicknesses. For one sample we compare the TOF results with stationary photocurrent and photoluminescence (PL) measurements.

The paper is organized as follows. In Sec. II we give the sample parameters and review the TOF technique. Furthermore, the other experimental techniques are briefly described. A theoretical model for resonant tunneling in crossed electric and magnetic fields will be given in Sec. III. In Sec. IV the results of the TOF measurements are presented and compared with the theoretical calculations of Sec. III. The dynamical aspects are also discussed. In Sec. V we present the results of the photocurrent and PL experiments. A brief summary will be given in Sec. VI.

II. EXPERIMENT

Two SL's were investigated in this study, sample 1 containing 50 periods of 12.3 nm GaAs and 2.1 nm AlAs, and sample 2 with 40 periods of 9.0 nm GaAs and 4.0 nm AlAs. The SL and two significantly larger GaAs wells on each side of the SL are forming the intrinsic region of a p - i - n diode. The total structure of sample 2 is shown in Table I. The structure of sample 1 is identical except for the embedded SL. The samples were grown by molecular beam epitaxy on a (100)-oriented n^+ -GaAs substrate and processed into mesas with Ohmic contacts of Cr/Au on the top and AuGe/Ni on the substrate side. The mesa diameter varied between 120 and 230 μm , corresponding to an area of 1.1×10^{-4} and 4.0×10^{-4} cm^2 . Under a reverse bias voltage V_A the applied electric field F_A in the SL is given by $F_A = (V_{\text{BI}} - V_A)/W$, where $V_{\text{BI}} = 1.52$ V is the built-in voltage and W the width of the intrinsic region. In reverse bias no carriers are injected via the contacts.

We employ time-dependent photocurrent measurements to study the vertical transport in these SL's in

a magnetic field applied parallel to the layers. The basic principles of the TOF technique are briefly reviewed. A thin sheet of carriers is excited near the p contact of the p - i - n diode by means of a short laser pulse. Due to the electric field applied in reverse bias the generated electrons drift across the whole intrinsic region giving rise to a photocurrent that decays when the electrons reach the n contact. Hole transport occurs on a much longer time scale than electron transport and will be neglected.¹² In our experiments we use a laser diode (Hamamatsu PLP-01) with a pulse width of 59 ps at a repetition rate of 10 MHz. The wavelength of the laser diode is fixed at 659 nm, leading to a penetration depth of 301 nm in bulk GaAs.¹³ At this wavelength no light is absorbed in $\text{Al}_{0.5}\text{Ga}_{0.5}\text{As}$ (Ref. 13) so that no additional current components are created in the contact layers.

The samples are mounted in the bore of an optical split-coil magnet on 50 Ω transmission lines which are connected to a 20 GHz sampling oscilloscope (Hewlett-Packard 54102B mainframe and 54121A test set) through wide bandwidth coaxial connectors and cables. The bias voltage is applied through a bias tee with a rise time of 28 ps (Picosecond Pulse Lab Model 5535). The overall rise time of our setup is about 300 ps which is mainly determined by the capacitance of the samples. For the measurements of sample 2 a broadband amplifier is used which increases the rise time to 700 ps.

In the experiments the maximum of the photocurrent transient I_{max} is recorded as a function of the applied voltage for various magnetic fields. Assuming a constant drift velocity for a given electric field the photocurrent amplitude I_{max} is related in the simplest model to the transport time τ through the SL by

$$\frac{1}{\tau} = \frac{I_{\text{max}}}{Q_0}, \quad (1)$$

where Q_0 is the charge of the generated electrons. Equation (1) is also obtained within the framework of a Gaussian transport model.^{11,12} In order to be able to apply Eq. (1) the total rise time has to be much smaller than any characteristic times of processes causing a reduction of the number of drifting carriers and thus a reduction of the photocurrent amplitude I_{max} . Since the recombination lifetime is ≈ 1 ns (Ref. 14) and the transport times are of the order of several ns this condition is fulfilled for both samples. For sample 1 we note that the integrated photocurrent (integrated over the first 45 ns after the laser pulse) starts to saturate for applied voltages < -3 V and shows a well defined plateau between -11 V and -14 V, followed by an increase due to avalanche multiplication at higher fields. We therefore identify the value of this plateau as the generated photocharge Q_0 . In order to avoid any space charge effects and screening of the applied electric field Q_0 is kept at a low value of 0.6 pC, corresponding to a surface charge density of less than 3×10^{10} cm^{-2} . Due to the thicker barriers the photocurrent transients of sample 2 are much longer than for sample 1 and therefore even at higher fields they are strongly affected by recombination losses. This inhibits an accurate determination of the generated charge Q_0 . However, for constant illumination intensities I_{max} is still

TABLE I. Total structure of sample 2.

n^+ -GaAs substrate		
100 nm	GaAs:Si	$n = 1 \times 10^{18} \text{ cm}^{-3}$
170 nm	$\text{Al}_x\text{Ga}_{1-x}\text{As:Si}$	$x = 0.0 \rightarrow 0.5$
300 nm	$\text{Al}_{0.5}\text{Ga}_{0.5}\text{As:Si}$	$n = 1 \times 10^{18} \text{ cm}^{-3}$
70 nm	$\text{Al}_x\text{Ga}_{1-x}\text{As:Si}$	$n \downarrow \quad x = 0.5 \rightarrow 0.0$
25 nm	GaAs	
4.0 nm	AlAs	} $\times 40$
9.0 nm	GaAs	
4.0 nm	AlAs	
25 nm	GaAs	
70 nm	$\text{Al}_x\text{Ga}_{1-x}\text{As:Be}$	$p \uparrow \quad x = 0.0 \rightarrow 0.5$
700 nm	$\text{Al}_{0.5}\text{Ga}_{0.5}\text{As:Be}$	$p = 2 \times 10^{18} \text{ cm}^{-3}$
60 nm	GaAs:Be	
	Be	δ doped
10 nm	GaAs:Be	

a measure of the inverse transport time $1/\tau$.

In addition to the TOF measurements we study the electric field dependence of the photocurrent and the integrated photoluminescence intensity under stationary conditions as a function of the applied magnetic field. These experiments are performed in a conventional superconducting magnet. An optical fiber is used to illuminate the sample in the bore of the magnet and to collect the PL. The static photocurrent measurements are performed at an intensity of 40 mW/cm^2 with a Ti-sapphire laser which is pumped by an Ar^+ laser. The wavelength is chosen to be 750 nm , corresponding to a penetration depth of 546 nm in bulk GaAs.¹³ This results in a rather homogeneous carrier distribution over the whole SL. The photocurrent-voltage (I - V) characteristics are recorded with a Hewlett Packard 4140B pA meter or a Keithley 236 Source Measure Unit. The photoluminescence spectra are obtained with a HeNe laser (633 nm) at a similar intensity using a standard experimental setup. All measurements were performed at temperatures between 1.5 K and 2.4 K .

III. THEORY

Without an applied magnetic field resonant tunneling in a SL occurs when subbands of adjacent wells are aligned by means of an electric field applied perpendicular to the layers. Thus an electron in the ground state (first subband) can resonantly tunnel into the second subband of the neighboring well at an electric field strength $F = (E_{C2} - E_{C1})/ed$ where d denotes the SL period. After a subsequent intersubband relaxation process resonant tunneling into the next well is possible (sequential resonant tunneling¹⁵).

In crossed electric and magnetic fields the tunneling resonances are shifted to higher electric field strengths. This can be qualitatively explained using semiclassical arguments. We take z as the direction perpendicular to the layers and choose the magnetic field to be parallel to the x axis. A carrier that travels the *tunneling distance* d from one well to the other picks up a momentum $\hbar k_y = eBd$ due to the Lorentz force. In the effective mass approximation (EMA) this corresponds to an energy $\Delta E = e^2 B^2 d^2 / 2m^*$ that is transferred from the z to the y direction. Therefore in order to maintain the resonance condition this energy transfer has to be compensated by an additional electric field $\Delta F = \Delta E / ed$. In this paper we will not follow these rather crude arguments but will employ a more rigorous treatment.

We first focus on the energy levels in the quantum well in a moderate magnetic field applied parallel to the layers. Due to the high barriers in a GaAs-AlAs SL the quantization is predominantly electrical and we therefore can describe the effect of the magnetic field on the energy levels using a perturbation approach. In the EMA and Landau gauge ($\mathbf{B} = \mathbf{e}_x B$) the energies are given in first-order perturbation theory by¹⁶

$$E = E_i + \frac{\hbar^2 k_x^2}{2m_i^*} + \frac{e^2 B^2}{2m_i^*} (\langle z^2 \rangle_i - \langle z \rangle_i^2) + \frac{1}{2m_i^*} (\hbar k_y + eB \langle z \rangle_i)^2, \quad (2)$$

where E_i denotes the subband energy and m_i^* the parallel effective mass of the i th subband. The third term on the right hand side of Eq. (2) is the diamagnetic shift while the last term reflects the coupling of momentum $\hbar k_y$ to the motion in the z direction due to the Lorentz force. Thus the parallel magnetic field leads to a parabolic energy dispersion perpendicular to the layers with a minimum for each well and subband being characterized by the constraint

$$k_y |_{\min} = -\frac{eB}{\hbar} \langle z \rangle_i. \quad (3)$$

The resonant tunneling process between the first and second electronic subbands of adjacent wells in crossed electric and magnetic fields is illustrated in Fig. 1. A carrier that has relaxed to the minimum of the first electronic subband in the right well can resonantly tunnel into the left well when the parabolic dispersion of the second subband intersects this minimum. This occurs when an additional electric field ΔF is applied with respect to the zero magnetic field case. The corresponding energy shift $\Delta E = \Delta F ed$ is easily obtained making use of Eqs. (2) and (3):

$$\Delta E = \frac{e^2 B^2}{2m_2^*} (\langle z_r \rangle_1 - \langle z_l \rangle_2)^2 + \frac{e^2 B^2}{2m_2^*} (\langle z_l^2 \rangle_2 - \langle z_l \rangle_2^2) - \frac{e^2 B^2}{2m_1^*} (\langle z_r^2 \rangle_1 - \langle z_r \rangle_1^2), \quad (4)$$

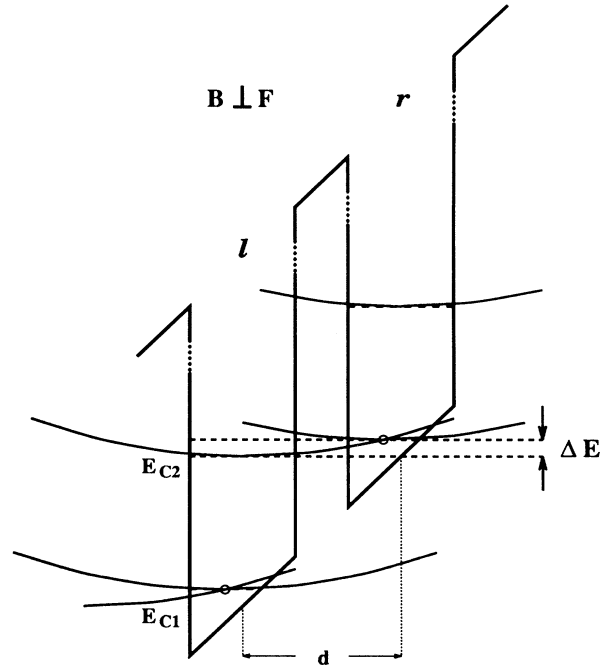


FIG. 1. Energy levels of a SL in crossed electric and magnetic fields. The first subband of the right well (r) is at resonance with the second subband of the left well (l). The shift of the resonance ΔE with respect to $B = 0 \text{ T}$ is not shown to scale.

where r and l denote the left and right wells in Fig. 1, respectively. The first term in Eq. (4) originates from the momentum transfer due to the Lorentz force, whereas the last two terms reflect the difference in the diamagnetic shifts of the involved subbands. We note that the expectation values in Eq. (4) depend on the electric field strength due to the quantum-confined stark effect (QCSE).¹⁷ The subsequent relaxation process now takes place not only between subbands but also involves a momentum relaxation in order to fulfill Eq. (3) in the left well.

IV. TIME-OF-FLIGHT MEASUREMENTS

We employ the TOF technique to study the resonance between the first and second electronic subbands in both samples in a parallel magnetic field. In this experiment the transport at resonance is governed by sequential resonant tunneling.^{10–12} We can therefore investigate how the dynamics of the resonant tunneling process is affected by the magnetic field.

In Fig. 2 we plot the normalized photocurrent amplitude I_{\max}/Q_0 as a function of the applied voltage $V_A = -F_A W + V_{BI}$ for sample 1. In the magnetic field the resonance is clearly shifted to larger reverse bias, thus higher electric fields. In Fig. 3 the absolute shift of the resonance is plotted as a function of the square of the magnetic field strength. We observe the expected linear relationship and obtain a slope of $(1.55 \pm 0.05) \times 10^{-2} \text{ V T}^{-2}$. To convert this value into an energy shift we use the following calibration procedure.

At 0 T we observe the resonance at -3.60 V . From photocurrent spectroscopy measurements we determine the subband spacing $E_{C2} - E_{C1}$ at this applied voltage to be $86(\pm 1) \text{ meV}$. The electric field at resonance is then given by $F_{\text{res}} = 86 \text{ meV}/d = 59.7 \text{ kV/cm}$. To check the consistency we employ a double quantum well model and numerically evaluate the subband spacing at this electric field strength. We obtain 85.5 meV in good agreement

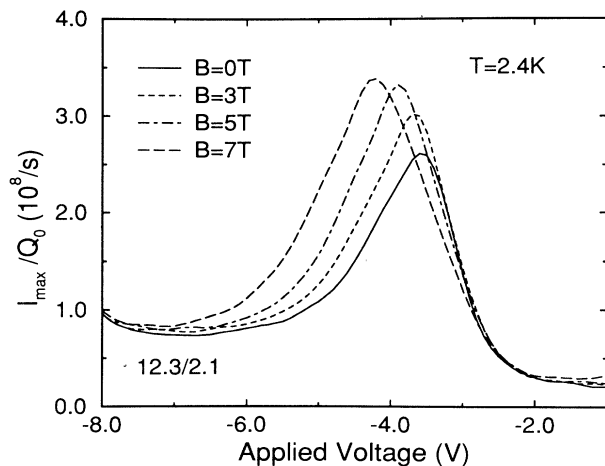


FIG. 2. Normalized photocurrent amplitude I_{\max}/Q_0 vs applied voltage in sample 1 for several magnetic field strengths.

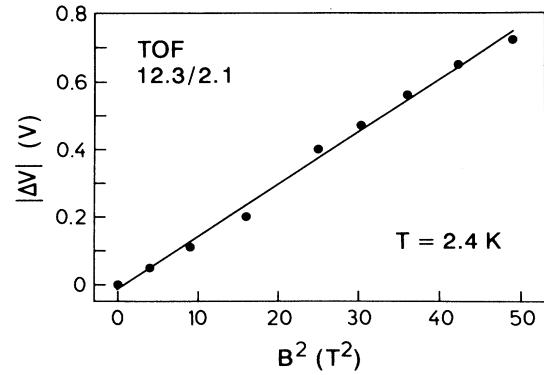


FIG. 3. Absolute shift ΔV of the resonance position vs the square of the magnetic field in sample 1.

with the experimentally determined value. Therefore we are confident about our voltage-energy calibration. The voltage shift for sample 1 then corresponds to $\Delta E/B^2 = (2.60 \pm 0.09) \times 10^{-4} \text{ eV T}^{-2}$.

In Fig. 4 we plot the normalized photocurrent amplitude of sample 2 versus the applied voltage for various magnetic fields. The 0 T resonance occurs at an applied voltage of -4.65 V . The subband spacing determined from photocurrent spectroscopy measurements at this voltage is $139(\pm 1) \text{ meV}$. Therefore the electric field strength at resonance is given by $F_{\text{res}} = 139 \text{ meV}/d = 106.9 \text{ kV/cm}$. The double quantum well model yields a value of 140 meV for the subband spacing at this field strength which again is in good agreement with the experimental result. The absolute shift of the resonance position for sample 2 is plotted in Fig. 5 as a function of B^2 . The shift is again quadratic in B and we obtain a slope of $(9.2 \pm 0.4) \times 10^{-3} \text{ V T}^{-2}$ corresponding to $\Delta E/B^2 = (2.07 \pm 0.09) \times 10^{-4} \text{ eV T}^{-2}$.

We now compare the experimental results with theoretical models. In the simplest approach the small difference in the diamagnetic shift of the two subbands and

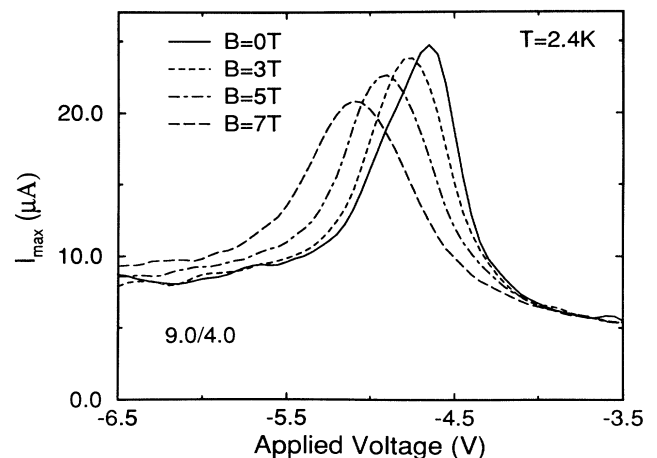


FIG. 4. Photocurrent amplitude I_{\max} vs applied voltage in sample 2 for several magnetic field strengths.

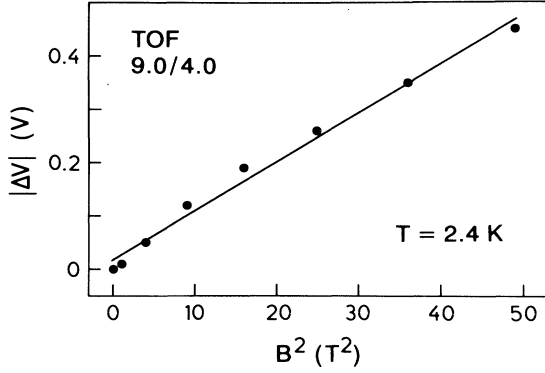


FIG. 5. Absolute shift ΔV of the resonance position vs the square of the magnetic field in sample 2.

the polarization of the wave functions due to the QCSE may be neglected. We may also ignore the difference in the parallel masses of the two subbands by setting m_1^* and m_2^* equal to m^* . Equation (4) then reduces to the semiclassical result $\Delta E = e^2 B^2 d^2 / 2m^*$. Taking m^* to be the bulk GaAs effective mass ($0.0665m_0$) we obtain $\Delta E/B^2 = 2.74 \times 10^{-4} \text{ eV T}^{-2}$ for sample 1 and $\Delta E/B^2 = 2.23 \times 10^{-4} \text{ eV T}^{-2}$ which are already in close agreement with the experimental values, but in both cases are larger than the experimental ones. To take into account the QCSE we numerically calculate the wave functions and compute the expectation values $\langle z \rangle$ and $\langle z^2 \rangle$ in Eq. (4) for the respective electric field values at resonance. This leads to $\Delta E/B^2 = 2.38 \times 10^{-4} \text{ eV T}^{-2}$ for sample 1 and $\Delta E/B^2 = 2.03 \times 10^{-4} \text{ eV T}^{-2}$ for sample 2 and results in very good agreement with the experimentally determined values. However, in particular in sample 2 conduction band nonparabolicities should also be considered. To evaluate the parallel subband masses m_i^* in Eq. (4) we use the expression derived from $\mathbf{k} \cdot \mathbf{p}$ perturbation theory¹⁸

$$\frac{1}{m_i^*} = \frac{1}{m^*} \left(1 + K_2 \frac{E_i}{E_g} \right), \quad (5)$$

where m^* is again the bulk GaAs effective mass ($0.0665m_0$), E_i the subband energy, and E_g the energy gap in GaAs. The nonparabolicity parameter K_2 describes the fourth-order contribution to the band curvature and has been determined to be -1.2 from magneto-optic studies in GaAs quantum wells.¹⁹ We then obtain $\Delta E/B^2 = 2.18 \times 10^{-4} \text{ eV T}^{-2}$ for sample 1 and $\Delta E/B^2 = 1.73 \times 10^{-4} \text{ eV T}^{-2}$ for sample 2. These values agree within 16% with the experimental values. The fact that both values are considerably smaller than the experimental results may be attributed to an overestimate of the parallel mass of the second subband by Eq. (5). However, we note that the energy shift is very sensitive to the SL period d , which enters quadratically into Eq. (4). The experimental error arising from the electric field calibration is estimated to be less than 5% and consequently cannot account for the deviation.

We now discuss how the dynamics of the resonant tunneling process is affected by the parallel magnetic field.

In sample 1 we can immediately deduce from the normalized photocurrent amplitude the transport time through the SL by applying Eq. (1). It is apparent from Fig. 2 that the peak value of the photocurrent amplitude increases with magnetic field. This is consistent with the observation that the corresponding transients become shorter. This decrease of the transport times with magnetic field is followed by a subsequent saturation for $B > 5 \text{ T}$. This is shown in Fig. 6 where the transport times at resonance are plotted as a function of B^2 for another set of measurements performed on a different mesa structure of sample 1 than in Fig. 2. How can this dependence of the transport times on the magnetic field be understood? The tunneling time τ_{RT} for coherent resonant tunneling between adjacent wells can be deduced from the level splitting ε of the aligned subbands: $\tau_{\text{RT}} = h/2\varepsilon$. From a numerical solution of Schrödinger's equation for a symmetric double well in an electric field we obtain $\tau_{\text{RT}} = 3.4 \text{ ps}$ for zero magnetic field. This is equivalent to a transport time through the whole SL of $\approx 0.17 \text{ ns}$, which is about a factor 20 smaller than the observed one. Since the subband spacing is above the optical phonon energy the intersubband relaxation should be faster than 1 ps (Refs. 20 and 21) and therefore cannot account for the discrepancy. In fact Grahn *et al.*²² determined the intersubband scattering time to be 0.4 ps in sample 1. While there are strong arguments that the destruction of coherence due to collision and relaxation prolongs the tunneling time²³ other authors argue that thickness fluctuations are the major reason for the observed discrepancy between theory and experiment.²⁴ In our case these thickness fluctuations result in an inhomogeneous linewidth observed in PL spectroscopy which is about three times larger than the calculated energy splitting ε at resonance. Even though we are not able to determine which one of the above stated effects accounts most for the prolongation in our experiment, we, however, note the following. In both cases the tunneling rate $\Gamma_{\text{RT}} = 2\varepsilon/h$ at resonance is convoluted by a Lorentzian or a Gaussian, leading to a broadening of the resonance and reduction in the peak tunneling rate. The measured peak resonant tunneling time is then given by $\tau_{\text{RT}} = \gamma h/2\varepsilon$ with $\gamma > 1$. In the

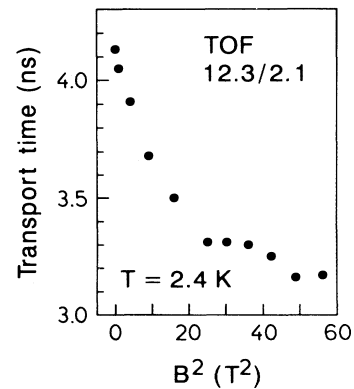


FIG. 6. Transport time through the SL vs the square of the magnetic field in sample 1.

parallel magnetic field the resonance is shifted to higher electric fields and therefore the effective barrier height at resonance is lowered. This results in an increase of the energy splitting ε . Thus a decrease of the resonant tunneling time is expected which is in agreement with the experiment. The observed saturation above 5 T is not fully understood at this point but may be related to the breakdown of the discussed resonant tunneling models in this sample at higher magnetic fields.

In sample 2 it is not possible to determine the absolute value of the transport times for the reasons stated in Sec. II. Nevertheless we can still deduce from the photocurrent amplitude I_{\max} how the transport at resonance is affected by the applied parallel magnetic field. From Fig. 7 it is evident that the peak value of the photocurrent amplitude decreases. This reduction of I_{\max} at resonance is almost linear with B^2 . This means that the resonant tunneling times in sample 2 increase with magnetic field, which seems to contradict the observation in sample 1. However, in sample 2 due to the thicker barriers the calculated energy splitting ε is negligible compared to any realistic value for the collision broadening of the energy levels. Therefore we cannot apply the resonant tunneling picture discussed above. From theoretical calculations on DBRTS's with thick barriers^{25,26} it is well known that the transmission probability for sequential resonant tunneling is significantly changed in a parallel magnetic field leading to a decrease of the current at resonance in these structures. We believe that the resonant tunneling time in sample 2 is prolonged for similar reasons.

V. I - V CHARACTERISTICS AND PL SPECTROSCOPY UNDER STATIONARY CONDITIONS

In contrast to the TOF measurements, where we monitor the transport of electrons through the whole SL, the structures in the I - V characteristics under stationary illumination arise from two competing processes: transport and recombination. This can be understood from Fig. 8 where for sample 2 the I - V trace and the inte-

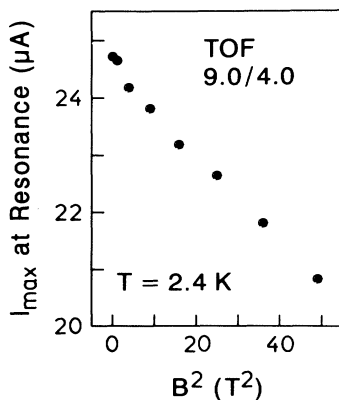


FIG. 7. Photocurrent amplitude I_{\max} at resonance vs the square of the magnetic field in sample 2.

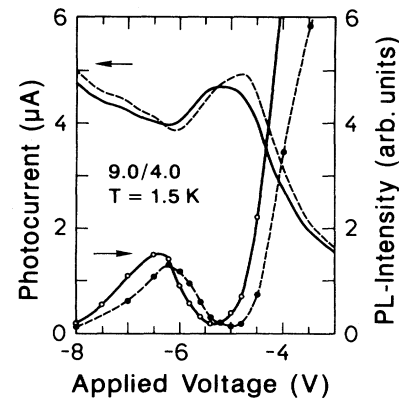


FIG. 8. Photocurrent and integrated PL intensity under stationary conditions vs applied voltage for 0 T (dashed lines) and 6 T (solid lines) in sample 2.

grated PL intensity are plotted as a function of the applied voltage at 0 T (dashed lines) and 6 T (solid lines). The peak in the I - V characteristics due to the $E_{C1} - E_{C2}$ resonance coincides with a minimum in the PL intensity since electrons and holes are more efficiently separated by the electric field at resonance than outside the resonance. For the zero magnetic field case this was already observed by Tarucha, Ploog, and von Klitzing²⁷ in weakly coupled GaAs-AlAs SL's. In sample 2 we can therefore use both the I - V characteristics and the PL intensity to study the effect of the magnetic field on the resonance position. However, in a more strongly coupled SL the transport times at higher fields become so short that recombination is negligible and almost all carriers are collected in the contact regions. The current then coincides with the generation rate and the I - V characteristics are structureless. For sample 1 this is the case for applied voltages below -3 V. Thus we cannot study resonant tunneling between E_{C1} and E_{C2} using stationary techniques in this sample at low excitation densities.

First we focus on the I - V trace and the PL intensity

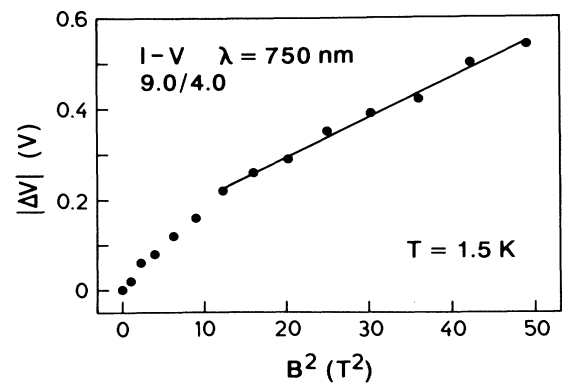


FIG. 9. Absolute shift ΔV of the resonance position vs the square of the magnetic field obtained from stationary photocurrent measurements in sample 2.

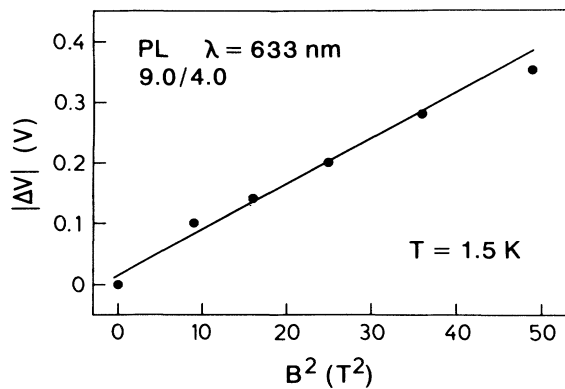


FIG. 10. Absolute shift ΔV of the resonance position vs the square of the magnetic field obtained from stationary PL measurements in sample 2.

plotted at 0 T in Fig. 8. We note that the resonances are broader and slightly shifted to higher electric fields in comparison to the TOF experiments of Fig. 4. This can be attributed to field inhomogeneities and screening due to the relatively large carrier concentration in the SL under cw excitation. In the case of the PL measurements excitonic effects may also be of importance.²⁸ Since the resonances are relatively broad an accurate determination of the resonance peak is rather difficult. However, in the magnetic field the expected shift of the resonance position to higher electric fields is observed. In Figs. 9 and 10 we plot the absolute shift of the resonance with respect to the 0 T case as a function of B^2 . For the I - V characteristics (Fig. 9) we obtain a steep increase at low magnetic fields and find a linear relationship with a slope of $(8.8 \pm 0.4) \times 10^{-3} \text{ V T}^{-1}$ thereafter. The anomaly on the low magnetic field side arises mainly from the fact that the shape of the resonance changes as it is shifted to larger reverse bias. For the PL intensity measurements (Fig. 10) we obtain a linear dependence on the square of the magnetic field and a slope of $(7.5 \pm 0.4) \times 10^{-3} \text{ V}$

T^{-1} . Both values deviate from the TOF results by 4% and 18%, respectively. The deviation can be attributed to field inhomogeneities and screening and to the inaccuracy in determining the resonance positions. We also note the decrease in the resonance peak amplitude with magnetic field (Fig. 8) which is consistent with the time-dependent measurements.

VI. SUMMARY

In this paper we have presented a comprehensive study on resonant tunneling in crossed electric and magnetic fields in two differently coupled GaAs-AlAs SL's. We have employed time-dependent photocurrent measurements to study how the dynamics of the tunneling process at resonance is affected by the magnetic field. Depending on the coupling of the SL the tunneling times at resonance are either decreased (strong coupling) or increased (weak coupling) with magnetic field which can be qualitatively explained. The shift of the resonance position is found to be proportional to the square of the magnetic field. Since we have a well defined energy-voltage relation in our samples we find good quantitative agreement with theoretical calculations taking into account the polarization of the wave functions due to the electric field. In the last section we have shown that in the weaker coupled sample stationary photocurrent and photoluminescence measurements can also be employed to study resonant tunneling in a parallel magnetic field. However, they are less precise methods in comparison to the time-dependent photocurrent experiment.

ACKNOWLEDGMENTS

We thank M. Hauser and A. Fischer for sample growth. We are grateful to K. Lier (U. Würzburg), A. P. Heberle, and A. J. Shields for valuable discussions. The work was supported in part by the Bundesminister für Forschung und Technologie (Project No. 01BM121/8).

¹L. Eaves, D.C. Taylor, J.C. Portal, and L. Dmowski, in *Two Dimensional Systems: Physics and New Devices*, edited by G. Bauer, F. Kuchar, and H. Heinrich, Springer Series in Solid-State Sciences Vol. 67 (Springer, Berlin, 1986), p. 96.

²B.R. Snell, K.S. Chan, F.W. Sheard, L. Eaves, G.A. Toombs, D.K. Maude, J.C. Portal, S.J. Bass, P. Claxton, G. Hill, and M.A. Pate, *Phys. Rev. Lett.* **59**, 2806 (1987).

³J. Smoliner, W. Demmerle, G. Berthold, E. Gornik, G. Weimann, and W. Schlapp, *Phys. Rev. Lett.* **63**, 2116 (1989).

⁴M.L. Leadbeater, L. Eaves, P.E. Simmonds, G.A. Toombs, F.W. Sheard, P.A. Claxton, G. Hill, and M.A. Pate, *Solid-State Electron.* **31**, 707 (1988).

⁵S. Ben Amor, K.P. Martin, J.J.L. Rascol, R.J. Higgins, A. Torabi, H.M. Harris, and C.J. Summers, *Appl. Phys. Lett.* **53**, 2540 (1988).

⁶M. Helm, F.M. Peeters, P. England, J.R. Hayes, and E. Colas, *Phys. Rev. B* **39**, 3427 (1989).

⁷M.L. Leadbetter, E.S. Alves, L. Eaves, M. Henini, O.H. Hughes, A. Celeste, J.C. Portal, G. Hill, and M.A. Pate, *J. Phys. Condens. Matter* **1**, 4865 (1989).

⁸L. Eaves, R.K. Hayden, D.K. Maude, M.L. Leadbetter, E.C. Valadares, M. Henini, O.H. Hughes, J.C. Portal, L. Cury, G. Hill, and M.A. Pate, in *High Magnetic Fields in Semiconductor Physics III*, edited by G. Landwehr, Springer Series in Solid-State Sciences Vol. 101 (Springer, Berlin, 1990), p. 645.

⁹T.M. Fromhold, F.W. Sheard, and G.A. Toombs, *Surf. Sci.* **228**, 437 (1990); T.M. Fromhold, F.W. Sheard, and G.A. Toombs, in *Proceedings of the 20th International Conference on the Physics of Semiconductors*, edited by E.M. Anastassakis and J.D. Joannopoulos (World Scientific, Singapore, 1990), p. 1250.

- ¹⁰H. Schneider, K. von Klitzing, and K. Ploog, *Europhys. Lett.* **8**, 575 (1989).
- ¹¹H. Schneider, K. von Klitzing, and K. Ploog, *Superlatt. Microstruct.* **5**, 383 (1990).
- ¹²H. Schneider, H.T. Grahn, and K. von Klitzing, *Surf. Sci.* **228**, 362 (1990).
- ¹³D.E. Aspnes, S.M. Kelso, R.A. Logan, and R. Bhat, *J. Appl. Phys.* **60**, 754 (1986).
- ¹⁴J. Feldmann, G. Peter, E.O. Göbel, P. Dawson, K. Moore, C. Foxon, and R.J. Elliot, *Phys. Rev. Lett.* **59**, 2337 (1987).
- ¹⁵F. Capasso, K. Mohammed, and A.Y. Cho, *Appl. Phys. Lett.* **48**, 478 (1986).
- ¹⁶J.K. Maan, in *Festkörperprobleme 27*, edited by P. Grosse (Vieweg, Braunschweig, 1987), p. 137.
- ¹⁷D.A.B. Miller, D.S. Chemla, T.C. Damen, A.C. Gossard, W. Wiegmann, T.H. Wood, and C.A. Burrus, *Phys. Rev. Lett.* **53**, 2173 (1984).
- ¹⁸E.D. Palik, G.S. Picus, S. Teitler, and R.F. Wallis, *Phys. Rev.* **122**, 475 (1961).
- ¹⁹D.C. Rogers, J. Singleton, R.J. Nicholas, C.T. Foxon, and K. Woodbridge, *Phys. Rev. B* **34**, 4002 (1986).
- ²⁰M.C. Tatham, J.F. Ryan, and C.T. Foxon, *Phys. Rev. Lett.* **63**, 1637 (1989).
- ²¹J.K. Jain and S. Das Sarma, *Phys. Rev. Lett.* **62**, 2305 (1989); R. Ferreira and G. Bastard, *Phys. Rev. B* **40**, 1074 (1989).
- ²²H.T. Grahn, H. Schneider, W.W. Rühle, K. von Klitzing, and K. Ploog, *Phys. Rev. Lett.* **64**, 2426 (1990); H.T. Grahn, M.G.W. Alexander, and K. Ploog, in *Proceedings of the 20th International Conference on the Physics of Semiconductors*, edited by E.M. Anastassakis and J.D. Joannopoulos (World Scientific, Singapore, 1990), p. 1097.
- ²³J. Shah, K. Leo, D.Y. Oberli, T.C. Damen, D.A.B. Miller, and J.P. Gordon, in *Proceedings of the 20th International Conference on the Physics of Semiconductors*, edited by E.M. Anastassakis and J.D. Joannopoulos (World Scientific, Singapore, 1990), p. 1222; K. Leo, J. Shah, J.P. Gordon, T.C. Damen, D.A.B. Miller, C.W. Tu, and J.E. Cunningham, *Phys. Rev. B* **42**, 7065 (1990).
- ²⁴W.W. Rühle, in *Proceedings of the 20th International Conference on the Physics of Semiconductors*, edited by E.M. Anastassakis and J.D. Joannopoulos (World Scientific, Singapore, 1990), p. 1226.
- ²⁵F. Ancilotto, *J. Phys. C* **21**, 4657 (1988).
- ²⁶G. Platero and C. Tejedor, in *High Magnetic Fields in Semiconductor Physics III*, edited by G. Landwehr, Springer Series in Solid-State Sciences Vol. 101 (Springer, Berlin, 1990), p. 664.
- ²⁷S. Tarucha, K. Ploog, and K. von Klitzing, *Phys. Rev. B* **36**, 4558 (1987).
- ²⁸H. Schneider, J. Wagner, and K. Ploog, *Phys. Rev. B* (to be published).